Activity-based protein profiling in methicillin-resistant staphylococcus aureus reveals the broad reactivity of a carmofur-derived probe

Uddin, M.J.; Overkleeft, H.S.; Lentz, C.S.

ChemBioChem

Research Article
doi.org/10.1002/cbic.202300473

Chemistry
Europe
European Chemical
Societies Publishing

www.chembiochem.org

Activity-Based Protein Profiling in Methicillin-Resistant *Staphylococcus aureus* Reveals the Broad Reactivity of a Carmofur-Derived Probe

Md Jalal Uddin,[a] Hermen S. Overkleeft,[b] and Christian S. Lentz*[a]

Activity-based protein profiling is a powerful chemoproteomic technique to detect active enzymes and identify targets and off-targets of drugs. Here, we report the use of carmofur- and activity-based probes to identify biologically relevant enzymes in the bacterial pathogen *Staphylococcus aureus*. Carmofur is an anti-neoplastic prodrug of 5-fluorouracil and also has antimicrobial and anti-biofilm activity. Carmofur probes were originally designed to target human acid ceramidase, a member of the NTN hydrolase family with an active-site cysteine nucleophile. Here, we first profiled the targets of a fluorescent carmofur probe in live *S. aureus* under biofilm-promoting conditions and in liquid culture, before proceeding to target identification by liquid chromatography/mass spectrometry. Treatment with a carmofur-biotin probe led to enrichment of 20 enzymes from diverse families awaiting further characterization, including the NTN hydrolase-related IMP cyclohydrolase PurH. However, the probe preferentially labeled serine hydrolases, thus displaying a reactivity profile similar to that of carbamates. Our results suggest that the electrophilic *N*-carbamoyl-5-fluorouracil scaffold could potentially be optimized to achieve selectivity towards diverse enzyme families. The observed promiscuous reactivity profile suggests that the clinical use of carmofur presumably leads to inactivation of a number human and microbial enzymes, which could lead to side effects and/or contribute to therapeutic efficacy.

Introduction

Activity-based protein profiling (ABPP) uses functionalized active-site directed small molecule probes known as activity-based probes (ABPs) to selectively label active enzymes, which can then be detected, identified and quantified through various analytical methods. A broad variety of probes has been designed to target diverse enzyme families and the application range spans from identification of drug targets and off-targets by chemical proteomics[1] to in vivo imaging or single-cell imaging studies in diverse organisms as extensively reviewed elsewhere.[2–6]

Some probes have been designed to target enzyme families in the broadest possible way[7] and have been applied for profiling studies in diverse organisms, whereas other probes have primarily been designed and validated for interaction with a particular target in a certain organism of interest. Repurposing these probes and validating their potential interactions with as of yet unidentified targets in other biological specimen may provide a short-cut for the discovery and functional validation of previously uncharacterized enzymes.
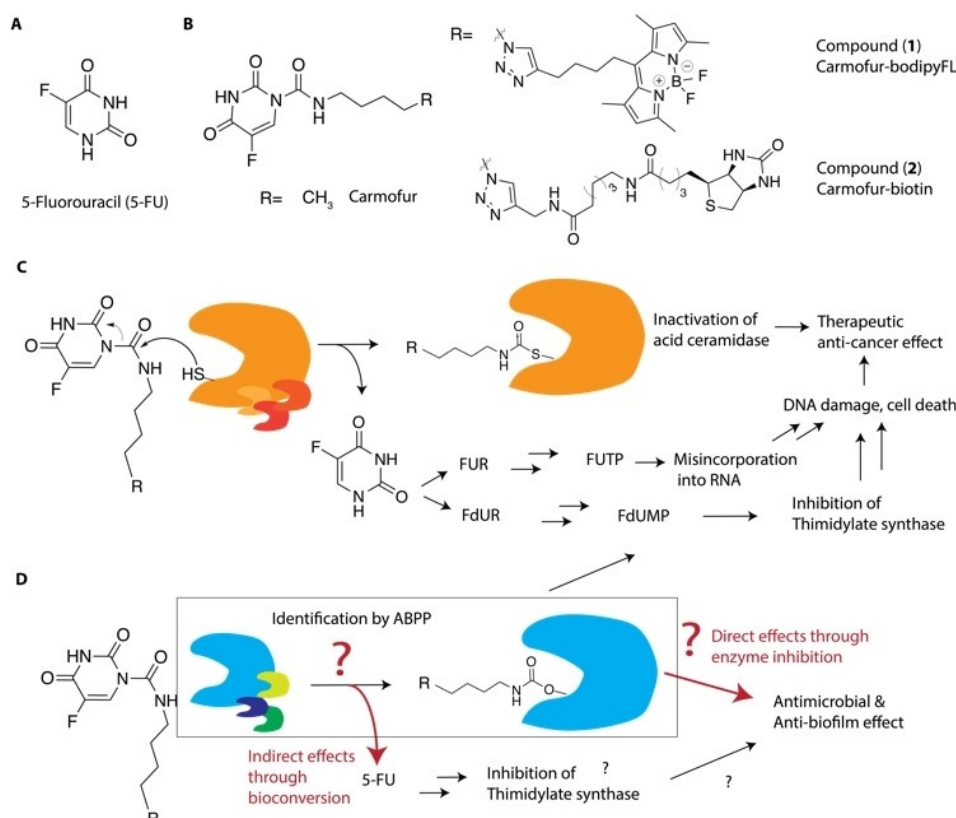
One focus of our research has been the characterization of new enzyme activities in bacterial pathogens. In a previous ABPP-study we have used fluorophosphonate probes to identify ten uncharacterized serine hydrolases in the bacterial pathogen *Staphylococcus aureus* that have emerging roles in pathogenesis and as potential anti-virulence targets.[8] In an ongoing effort to expand this work we seek to characterize the activity of additional enzyme families that are not well characterized. One interesting candidate for this approach are carmofur-derived probes (Scheme 1) that were generated to target human acid ceramidase (ACase)[9] after carmofur had been identified as a potent inhibitor of ACase.[10] Carmofur, or 1-hexylcarbamoyl-5-fluorouracil, is a registered anti-neoplastic drug for treatment for colorectal cancer in several countries[11,12] and a number of other potential therapeutic applications are under investigation as summarized in a recent review.[13] Carmofur is a prodrug of the antimetabolite 5-fluorouracil (5-FU) and its bioconversion pathways and known mechanism of action are illustrated in Scheme 1C. In human cells, 5-FU is converted to various bioactive metabolites that, in a complex mechanism, ultimately result in DNA damage and cell death.[14,15] The bioactive 5-FU-derived metabolites include, for example, fluorodeoxyuridine monophosphate, which inhibits thymidylate synthase, and fluorouridine triphosphate, which is irregularly incorporated into RNA.[12,15] Whereas carmofur had originally been designed as a prodrug, it has been shown that this compound retains activity against 5-FU-resistant cancers, suggesting involvement

[a] M. J. Uddin, Prof. Dr. C. S. Lentz
     Department of Medical Biology
     UiT- The Arctic University of Norway
     9019 Tromsø (Norway)
     E-mail: christian.s.lentz@uit.no

[b] Prof. Dr. H. S. Overkleeft
     Department of Bioorganic Synthesis
     Leiden Institute of Chemistry, Leiden University
     Einsteinweg 55, 2333 CC Leiden (The Netherlands)

ChemBioChem

Research Article
doi.org/10.1002/cbic.202300473

Chemistry
Europe
European Chemical
Societies Publishing

Scheme 1. Chemical structures of compounds used in this study. A) 5-FU. B) Carmofur and related probes carmofur-bodipyFL (**1**) and carmofur-biotin (**2**). C) Bioconversion of carmofur and 5-FU in humans and mechanism of action; FUR: fluorouridine, FdUR: fluorodeoxyuridine, FUTP: fluorouracil triphosphate, FdUMP: fluorodeoxyuridine monophosphate. D) Schematic illustration of the bioconversion pathway and mechanism of action underlying the antimicrobial and anti-biofilm effects of carmofur in *S. aureus*. Enzymes identified by ABPP could directly contribute to the biological effects and/or indirectly have relevance for the bioconversion to 5-FU as indicated by red font and arrows. Whereas (C) shows the presumed inactivation mechanism of carmofur through carbamoylation of the active-site Cys nucleophile of the cysteine amidase ACase, (D) illustrates the proposed carbamoylation of active-site Ser of serine hydrolases, which this study determined as the major target class of carmofur probes in *S. aureus*.

of additional targets not shared with 5-FU, such as ACase[16–18] (Scheme 1C).

ACase is a cysteine amidase belonging to the N-terminal nucleophile (NTN) hydrolase family and catalyzes the hydrolysis of ceramide to sphingosine and free fatty acids, which is the last step in the lysosomal degradation of (glycol)sphingolipids. Deficiency in ACase causes the lysosomal storage disorder Farber disease.[19] In another lysosomal storage disease, Gaucher Disease, a deficiency in glucocerebrosidase leads to an accumulation in glucosylceramide which is a potential substrate of ACase. Intriguingly, a fluorescent carmofur probe has been used to quantify ACase levels in human tissue extracts, thus revealing higher levels of ACase activity in splenic tissues from Gaucher disease patients compared to tissues from a healthy control group.[9]

Interestingly, carmofur and its parent drug 5-FU have been shown to exhibit general antimicrobial as well as antibiofilm activity against various bacteria including methicillin-resistant *S. aureus* (MRSA).[20,21] The mechanism behind the antimicrobial activity of 5-FU in bacteria is not well understood, but believed to be connected to inhibition of thymidylate synthase and a resulting blockade of DNA synthesis.[22] The anti-biofilm and virulence-attenuating activities in several species have been connected with competition with regulatory functions of uracil[23] and interference with quorum sensing.[24,25] The mechanism underlying the antimicrobial activity of carmofur has not been investigated. We hypothesized that, in analogy to the contribution of ACase inhibition to the therapeutic effect of carmofur in human, microbial enzymes targeted by carmofur might directly contribute to the antimicrobial and anti-biofilm effects of the drug and/or contribute to the bioconversion of carmofur to 5-FU.

In this study, we therefore applied carmofur-derived ABPs to profile enzymatic targets of this drug in MRSA. Because members of the NTN hydrolases family, which carmofur targets in human, are poorly characterized in bacteria, we hypothesized that this approach would be suitable to identify novel enzymes of this family with relevant biological functions. Our study revealed that, in addition to NTN hydrolases, carmofur interacts with a diversity of bacterial enzymes, particularly serine hydrolases. We demonstrate that lack of several individual target enzymes does not affect the susceptibility of *S. aureus* to carmofur and propose that these enzymes collectively contribute to the bioconversion of this drug to 5-FU and might also play a role for its anti-biofilm activity. Our study also has important implications regarding the use of carmofur in the

clinic, since it suggests that the drug might inactivate a similarly broad range of enzymes in humans as well as the human gut microbiome, which may affect the therapeutic outcome and cause side-effects.

Results and Discussion

Gel-based activity-based protein profiling by using a fluorescent carmofur probe

We conducted initial ABPP studies with the fluorescent carmofur-derived ABP (**1**) on live *S. aureus* cells (clinically relevant methicillin-resistant strain USA300 JE2) that were grown under biofilm-promoting growth conditions on tryptic soy agar supplemented with 100 mM $MgCl_2$ (TSAMg) in analogy to previous studies.[8] After labeling, cells were lysed and labeled proteins resolved by SDS-PAGE analysis and visualized by in-gel fluorescence scanning. We observed that the carmofur probe indeed led to dose-dependent labeling of certain *S. aureus* proteins (Figure 1). Two species corresponding to a molecular weight of >52 kD were most potently labeled (with bands apparent already at a probe concentration of 100 nM). Several additional bands with a molecular weight of around 31, 38, 54, 58, and 76 kDa, respectively, were labeled at 1 µM (Figure 1A). Since bacteria are expected to produce different enzymes depending on their growth environment, we compared the labeling profile of bacteria grown on TSAMg with that of bacteria grown to stationary phase in liquid culture using a standard rich cultivation medium (tryptic soy broth, TSB; Figure 1B). To differentiate secreted proteins that accumulate over the course of liquid cultivation from cell-associated proteins, we separated cells from the culture media that contains secreted proteins by centrifugation for differential analysis. We observed three dominant bands in the culture supernatant, whereas several proteins were detected in the cell pellet (Figure 1B).

To address whether the observed labeling profile achieved under biofilm-promoting conditions is the result of specific active-site directed interactions, we investigated if pre-incubation with the unlabeled parent inhibitor carmofur could block labeling of the fluorescent carmofur probe **1** in a competitive ABPP setup. Indeed, pre-incubation with carmofur (3–30 µM) led to reduced labeling of three of the most pronounced bands at 31, 38, and 54 kDa, suggesting that carmofur can compete with ABP (**1**). In contrast, pre-incubation with 5-FU, which is not expected to irreversibly interact with any of the targets, did not lead to alterations in the ABP-labeling patterns up to a concentration of 30 µM.

We suspected that the alterations in the labeling profile at high concentrations of 5-FU might be due to nonspecific effects related to its antimicrobial activity rather than competition labeling. We therefore determined the Minimum inhibitory concentrations (MICs) of the inhibitors carmofur and 5-FU against *S. aureus* USA300 JE2, which were both 5 µM. Thus, specific competition of carmofur with the targets of **1** becomes evident at sub-MIC concentrations, supporting the specific nature of these interactions. For 5-FU, in contrast, the changes in the labeling profile are seen at concentrations six times higher than its MIC (Figure 1C) and therefore most likely result nonspecifically from its antimicrobial activity rather than from specific competition with the probe.
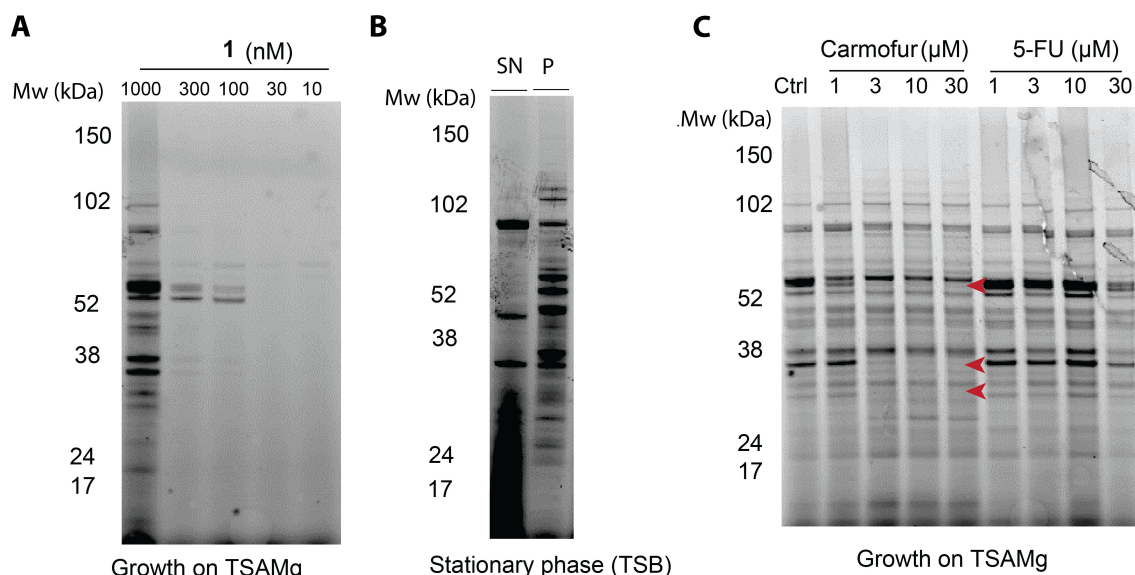
Figure 1. Fluorescent ABP-labeling profiles of *S. aureus* USA300 JE2 with carmofur probe **1**. Live bacteria were labeled with different concentrations of probe **1** for 60 min at 37 °C before cells were lysed, and samples were subjected to SDS-PAGE analysis. All graphs show fluorescent scans in the Cy2 (488 nm) channel on an Amersham™ Typhoon™ 5 (Cytiva). A) Dose-dependent labeling profile of *S. aureus* USA300 JE2 cells harvested from TSAMg with probe **1** and B) labeling profile of *S. aureus* USA300 JE2 cell fractions from the stationary phase in liquid culture with probe **1** (1 µM); SN: culture supernatant, P: cell pellet. C) Competitive ABPP. Cells were pre-incubated with carmofur or 5-FU at the indicated concentrations for 60 min before the addition of probe **1** (1 µM). Arrowheads indicate bands with consistently reduced labeling after pre-incubation with carmofur.

ChemBioChem

Research Article
doi.org/10.1002/cbic.202300473

**Chemistry
Europe**
European Chemical
Societies Publishing

Target Identification

A limitation of the gel-based approach using fluorescent ABPs is that only the most abundant targets are detected and that their identity remains undefined. To overcome these shortcomings, we switched to using the biotin-tagged probe (**2**) in combination with a chemoproteomic workflow. It should be noted, however, that also this approach focuses on covalently bound targets and less stable, reversible interactions may be overlooked. In brief, live bacteria were grown under biofilm-promoting conditions on TSAMg before labeling with the biotin-tagged ABP (**2**) or carmofur as a control, lysed, and enriched for biotinylated proteins using a streptavidin resin. Samples were then analyzed by LC–MS/MS. Although the probe was used at 2 μM, which is lower than the MIC of carmofur (5 μM), we reasoned that its biological effects may still induce nonspecific changes to the general proteome that could translate to changes in the enrichment and detection of nonspecifically enriched "background" proteins in the probe-treated versus untreated chemoproteomic dataset. To account for such false positives, we decided to treat the unlabeled control sample with an equal concentration of carmofur. Treatment with carmofur-biotin (**2**) resulted in significant enrichment (p value < 0.05, enrichment > 1.5-fold) of 23 proteins compared to the carmofur-treated control dataset (Supporting Dataset 1, data are available from ProteomeXchange with identifier PXD043275). These 23 enriched proteins included 20 putative enzymes with diverse annotations (12 hydrolases or transferases, three oxidoreductases, three lyases, one isomerase, one putative chaperone-like protein; Table 1) as well as three non-enzymatic proteins that are likely false positives.

We identified one enzyme with structural similarity to the NTN hydrolase family,[29,30] the multifunctional PurH.[26] Featuring inosine 5'monophosphate (IMP) cyclohydrolase and 5-amino-imidazole-4-carboxamide ribonucleotide (AICAR) formyltransferase domains, this enzyme has a dual role in de novo purine synthesis.[26] Canonical members of the NTN hydrolase superfamily undergo self-processing to eliminate an N-terminal polypeptide, resulting in the active enzyme with a Ser, Thr or Cys nucleophile at the new N-terminus.[27,30] The bifunctional PurH however possesses an NTN-like fold, but the putative binding site with the corresponding nucleophile responsible for covalent binding to the carmofur probe remains to be identified.

The enzyme family for which the highest number of members were enriched by the carmofur probe **2** were serine hydrolases. This includes 3 α,β-hydrolases, the fluorophosphonate-binding hydrolases (FphB, FphC, and FphF) that we have described recently and which share a conserved Ser-His-Asp catalytic triad with serine as the active site nucleophile.[8,28] We also identified additional hydrolases/transferases that are annotated with a serine in the active site: the putative O-acetyltransferase Oat with an annotated SGNH-hydrolase-type esterase domain and the teichoic acid D-Ala esterase FmtA, which harbors a β-lactamase domain with a conserved catalytic triad of Ser-Lys-Asp. FmtA catalyzes the hydrolytic removal of D-

alanine esters on wall teichoic acid (WTA),[29,30] thereby regulating charge and integrity of the bacterial cell wall.

Among these serine hydrolase targets of carmofur, the only enzyme for which a substrate-bound crystal structure is available that could give indications on the molecular basis of binding of carmofur, is FphF.[28] FphF is a serine carboxylesterase with a broad substrate-selectivity profile against synthetic fluorogenic substrates. The enzyme had peak activity against a heptanoate-based substrate and the crystal structure showed that the C7 acyl chain fully occupied the hydrophobic acyl binding pocket of FphF.[28] We propose that carmofur binding leads to carbamoylation of the active site serine and assume that the hexyl-carbamoyl group of carmofur, which has a similar chain length to the C7 acyl of the preferred substrate, fits well into the acyl binding pocket. Since the partially open architecture of the acyl binding pocket of FphF can also accommodate substrates with longer acyl chains (although with poorer fits in docking studies) with terminal atoms pointing out of the pocket,[28] this provides a molecular basis for binding of the longer carmofur-derived probes. The observed promiscuity and reactivity toward serine hydrolases concurs with a recent report identifying carmofur as an inhibitor of another N-terminal cysteine hydrolase (N-acylethanolamine acid hydrolase), as well as of a human serine hydrolase (fatty acid amide hydrolase).[31] We therefore conclude that the carbamoyl-5-flurouracil electrophile elicits a similar reactivity profile to carbamates, which are known inhibitors of serine hydrolases.[32]

The molecular basis and specificity of the interactions of the carmofur probes with the diverse other enriched enzymes such as lyases, oxidoreductases or metal-dependent hydrolases within part unknown or even without predicted active site nucleophiles (as indicated in Table 1), remains to be determined.

Gel-based target validation

To validate the chemoproteomic results and to assign the bands identified in gel-based ABPP, we performed gel-based labeling studies using transposon mutants deficient in targets identified by MS, with a focus on the NTN and serine hydrolases. As we detected several Fph enzymes in the MS dataset, we first tested the entire panel of Fph A–H mutants and the secreted lipases SAL1 and −2 which was available from previous studies[8] in strain USA300 LAC. This allowed for a clear assignment of SAL2, FphB, FphE, FphF as labeled targets of the carmofur probe **1** (Figure 2A). Among the α,β-hydrolases some differences were apparent in the gel-based and MS-based studies: FphC was not detected by the gel-based approach, whereas SAL2 and FphE were detected on the gel, but not by MS. These differences could result from differences in permeability and activity of the fluorescent versus biotinylated probe. In the case of FphC this might also be due to limited resolution and lower sensitivity of gel-based ABPP. Interestingly, α,β-hydrolases also accounted for all fluorescently labeled bands that were detected after growth in liquid culture. SAL2 was found as the two dominant bands in the supernatant at around

ChemBioChem

Research Article
doi.org/10.1002/cbic.202300473

Chemistry
Europe
European Chemical
Societies Publishing

Table 1. Target enzymes of carmofur probe (2) in *S. aureus* USA300 JE2.

| Accession no.	Protein	Description	Active-site nucleophile/ putative site of attachment	Gene name	Unique peptides	Mol weight [kDa]	Abundance ratio: biotin/ctrl	Abundance ratio p value
QPB88705.1	FphF	carboxylesterase[28]	Ser	*est*A/*fph*F[8,28]	2	29.1	100.0	1×10^{-17}
WP_001146763.1	AhpD	alkyl hydroperoxide reductase	Cys	*ahp*D	5	16.5	10.0	7.34368×10^{-12}
QPB88396.1	YndB	SRPBCC domain-containing protein	unknown	*Ynd*B	2	20.1	5.8	0.0009
WP_001184005.1	AcuC	acetoin utilization protein	Lys	*acu*C	5	44.6	4.7	0.0036
WP_000379821.1	OatA	acetyltransferase	Ser	*oat*A	7	69.1	2.9	0.0008
QPB87247.1	PyrF	orotidine-5'-phosphate decarboxylase	Lys	*pyr*F	7	25.6	2.8	0.0257
WP_000058383.1	MaeB	NAD-dependent malic enzyme 4	Lys	*mae*B	3	44.2	2.6	0.0108
QPB88680.1	BetB	betaine-aldehyde dehydrogenase	Cys	*bet*B	3	54.6	2.2	0.0132
QPB86902.1	Eno	phosphopyruvate hydratase	Lys, Glu	*eno*	6	47.1	1.9	0.0243
QPB88514.1	ApbA	2-dehydropantoate 2-reductase	Lys, Glu	*apb*A	4	34.4	1.9	0.0322
WP_001178942.1	CshA	DEAD/DEAH box helicase	unknown	*csh*A	24	56.9	1.9	0.0099
QPB87344.1	FphC	hydrolase, α/β hydrolase fold family	Ser	SAUSA300_1194/ *fph*C[8]	9	35.2	1.7	0.0023
WP_001248939.1	YvcK	YvcK family protein	unknown	*yvc*K	5	36.2	1.7	0.0341
QPB87084.1	GNAT	GNAT family N-acetyltransferase	unknown	SAUSA300_0943	6	21.3	1.7	0.0294
QPB87049.1	YjbK	CYTH domain-containing protein	unknown (metal-dependent)	*yjb*K	2	23.4	1.7	0.0326
QPB86868.1	PepT	peptidase T	unknown (metal-dependent)	*pep*T	12	45.8	1.6	0.0224
WP_001281145.1	Alr	alanine racemase	Lys	*alr*	3	42.8	1.6	0.0105
QPB88602.1	FphB	Carboxylesterase[8]	Ser	SAUSA300_2473/*fph*B[8]	10	36.8	1.5	0.0388
QPB87101.1	FmtA	teichoic acid D-Ala esterase	Ser	*fmt*A	3	46	1.5	0.0390
QPB87118.1	PurH	IMP cyclohydrolase	Ser, Thr or Cys	*pur*H	26	54.3	1.5	0.0114

76 and >38 kDa (Figure 2B). SAL1 was associated to the cell pellet and appeared as diverse species of various molecular weight (Figure 2C). The only relevant remaining band in both fractions was assigned to the 31 kDa FphE (Figure 2B, C).

To account for the unidentified bands that can be detected in cells grown on TSAMg, we tested additional JE2-based mutants from the Nebraska Transposon Mutant Library (Figure 2D).[33] The *purH* transposon mutant, showed an altered labeling profile where several bands around and below the expected size of 54 kDa are missing (Figure 2D). It remains to be determined if the bands in question are all different fragments of PurH or if some of these changes may be attributed to secondary effects of the knock-out (Figure 2D). Certain ambiguity also remains regarding identification of the

46 kDa FmtA on the gel, as a band of this size was clearly reduced, but not absent (Figure 2D). In conclusion, these data confirm that the majority of the targets of the fluorescent carmofur probe in gel-based ABPP are indeed serine hydrolases.

Transposon mutations in abundant carmofur targets do not affect antimicrobial susceptibility to carmofur

Because the mechanism underlying the antimicrobial activities of carmofur is not properly documented, we aimed to determine if the enzymes enriched by the carmofur probe are relevant for the susceptibility to carmofur. Carmofur-binding to these targets could contribute to the antimicrobial effect
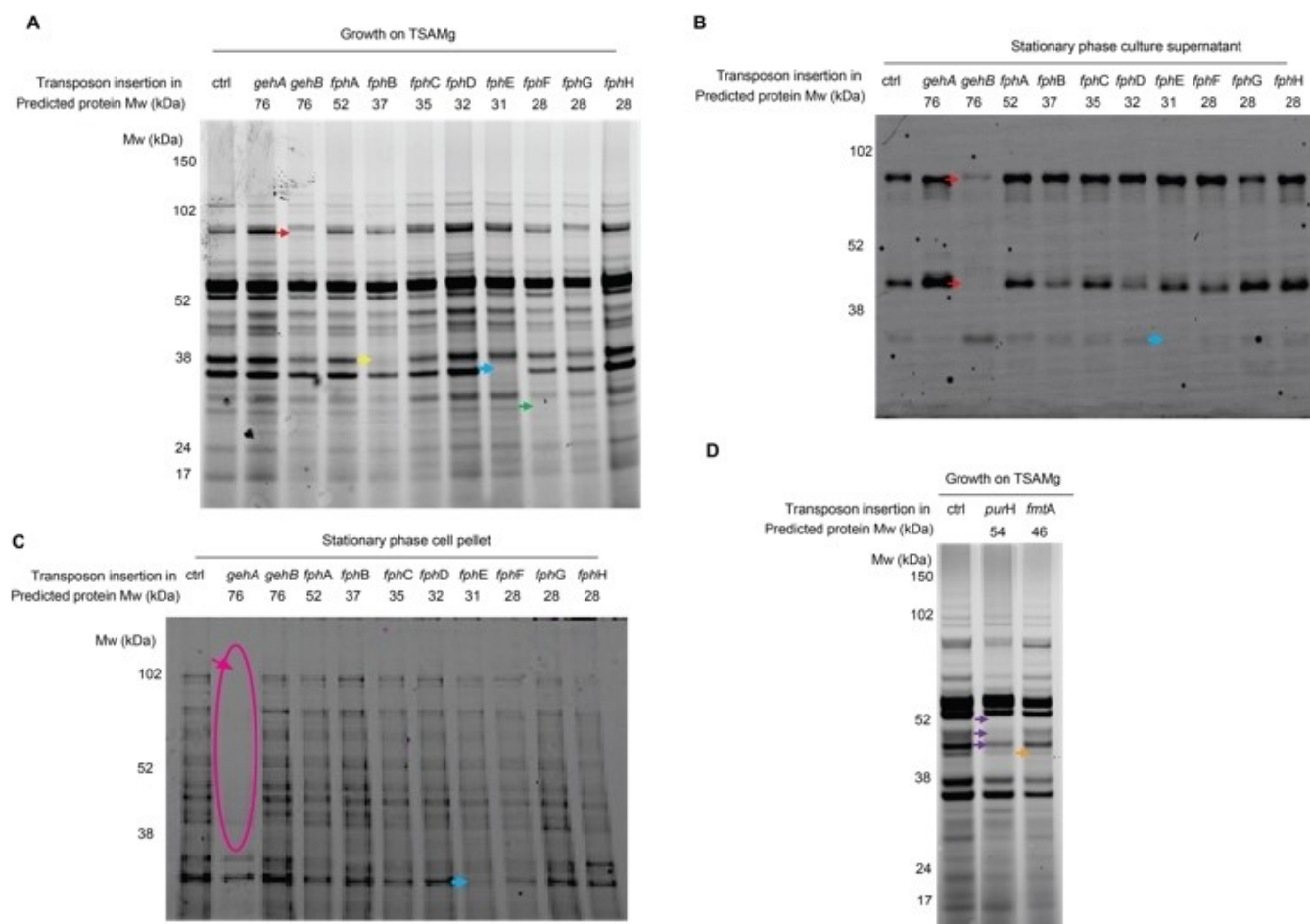
Figure 2. Fluorescent carmofur probe **1** labeling profiles of *S. aureus* USA 300 LAC transposon mutant strains with insertions of fluorophosphonate-binding hydrolases (Fphs) A–H and the secreted lipases SAL1 and −2 genes. The cells were labeled under two different conditions: A) cells grown in TSAMg and cells in stationary phase culture in TSB, fractionated into B) supernatant (SN) and C) cell pellet (P). D) Labeling profiles of *S. aureus* USA 300 JE2 transposon mutant strains with insertions of purine biosynthesis protein (*purH*) and teichoic acid D-Ala esterase (*FmtA*) genes. The cells were harvested in TSAMg. The labeled proteins disappearing in individual mutant strains are indicated by arrowheads.

directly (through target inhibition), but this is unlikely since none of the targets are essential. Alternatively, carmofur-binding can affect the antimicrobial activity indirectly by means of releasing 5-FU (Scheme 1D). Assuming that both the carmofur probes **1** and **2** and their parent drug lead to carbamoylation of the active site nucleophile (similar to ACase[9,18]) and the mode of action of carbamates on serine proteases,[32] these events will lead to release of 5-FU. We reasoned that, if activation of the prodrug was required, this could be reflected by slower bacterial killing by carmofur compared to 5-FU.

However, time-kill curve analysis revealed no differences in the kinetics of bactericidal effects elicited by 5-FU and carmofur (Figure 3). This suggests that either no conversion of carmofur to 5-FU is required, or more likely, that this conversion occurs very quickly. Unfortunately, there are – to the best of our knowledge–no available data on the biotransformation kinetics of carmofur to 5-FU in either bacteria, mammalian cells, humans, or animals that could help put these results into perspective.

We proceeded to determine the antimicrobial susceptibility of transposon mutant strains deficient in probe targets SAL1,
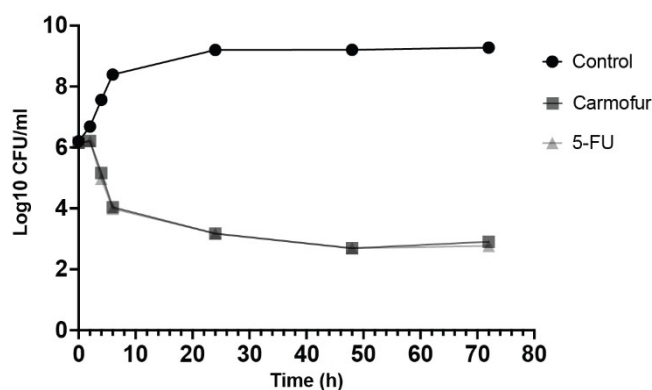
Figure 3. Time–kill curve analysis of carmofur and 5-FU. Stationary-phase *S. aureus* USA300 JE2 were treated with 4× the MIC of carmofur and 5-FU at 37 °C for 72 h. At various timepoints, aliquots were analyzed for CFU determination.

SAL2, FphB, FphC, FphE, FphF, PurH, or FmtA and their corresponding WT strains LAC or JE2 by broth microdilution testing. All strains showed an identical MIC of 5 μM. Our data

suggest that the activity of these enzymes individually does not affect the bactericidal activity of carmofur. Because the carmofur probe interacts promiscuously with a wealth of targets, it could be expected that they contribute collectively to the conversion of carmofur to 5-FU and that hence single knock-outs have only limited effects. It is also possible that other bacterial enzymes can hydrolyze carmofur to release 5-FU without being inactivated and labeled by the carmofur probes.

In contrast to the bactericidal activity, it seems plausible that inactivation of some of the identified enzymes may contribute to the anti-biofilm activities of carmofur.[21] PurH, for example, has already been attributed an important role in biofilm formation[34] and a putative involvement of other targets of the carmofur probe in biofilm formation merits further investigations.

Conclusions

This study has revealed the surprisingly broad reactivity profile of carmofur- and activity-based probes in the bacterial pathogen *S. aureus* and revealed the activity of a number of previously uncharacterized enzymes under biofilm-promoting conditions that merit further functional characterization. In addition to one expected member of the NTN hydrolase family, the IMP cyclohydrolase PurH, carmofur probes showed a similar reactivity to carbamates, in that they were able to interact with a number α,β-hydrolases and other serine hydrolases. Future studies might alter the electrophilic *N*-carbamoyl-5-fluorouracil scaffold in carmofur in order to generate more selective probes or inhibitors for some of the underexplored enzyme families targeted. In light of the clinical use of carmofur as a drug in colorectal cancer (as reviewed in ref. [13]) it must be considered that this drug might exhibit a similarly broad reactivity profile against human enzymes that could be potentially be related to both therapeutic and side effects. It is also plausible that carmofur reacts promiscuously with enzymes from human-associated microbiota. Considering the emerging knowledge of the impact gut microbiota have on human physiology, microbial (off−)targets could even be implicated in the mechanisms leading to its therapeutic effects. A prominent study has reported the impact of non-antibiotic drugs, including 5-FU, on human gut microbiota, even though the study concluded that the body concentration of 5-FU (in plasma) is lower than the concentration that reduces growth of at least one commensal bacteria by 25%.[35] However, in contrast to 5-FU, which is administered intravenously, carmofur is administered orally, thus making it very plausible that treatment leads to a concentration of carmofur in the human gut that is high enough to affect microbial enzymes.

Experimental Section

Bacterial strains and culture conditions: This work used *S. aureus* strains USA300 LAC, USA300 JE2 and their isogenic mutants as summarized in Table 2. All strains were routinely cultured on tryptic soy agar (TSA) or TSA with 100 mM MgCl$_2$ (TSAMg) or Difco tryptic

Table 2. Bacterial strains used in this study.

Strain	Description	Ref./source
S. aureus USA300 LAC	wild-type USA300 Los Angeles County (LAC) clone; multilocus sequence type 8, SCCmec type IV cured of antibiotic resistance plasmid	[41]
LAC_gehA: Tn	transposon insertion mutant in LAC SAU-SA300_2603 (SAL1); Ery^R, Linc^R	[8]
LAC_gehB: Tn	transposon insertion mutant in LAC SAU-SA300_0320 (SAL2); Ery^R, Linc^R	[8]
LAC_fphA: Tn	transposon insertion mutant in LAC SAU-SA300_2396 (fphA); Ery^R, Linc^R	[8]
LAC_fphB: Tn	transposon insertion mutant in LAC SAU-SA300_2473 (fphB); Ery^R, Linc^R	[8]
LAC_fphC: Tn	transposon insertion mutant in LAC SAU-SA300_1194 (fphC); Ery^R, Linc^R	[8]
LAC_fphD: Tn	transposon insertion mutant in LAC SAU-SA300_2148 (fphD); Ery^R, Linc^R	[8]
LAC_fphE: Tn	transposon insertion mutant in LAC SAU-SA300_2518 (fphE); Ery^R, Linc^R	[8]
LAC_fphF: Tn	transposon insertion mutant in LAC SAU-SA300_2564 (fphF); Ery^R, Linc^R	[8]
LAC_fphG: Tn	transposon insertion mutant in LAC SAU-SA300_1733 (fphG); Ery^R, Linc^R	[8]
LAC_fphH: Tn	transposon insertion mutant in LAC SAU-SA300 0763 (fphH); Ery^R, Linc^R	[8]
S. aureus USA300 JE2	a plasmid-cured derivative of USA300 LAC and Parent strain of Nebraska Transposon Mutant Library	[33]
JE2_purH: Tn	transposon insertion mutant in JE2 SAU-SA300_0975 (purH); Ery^R, Linc^R	[33]
JE2_fmtA: Tn	transposon insertion mutant in JE2 SAU-SA300_0959 (fmtA); Ery^R, Linc^R	[33]

soy broth (TSB). All bacterial strains were incubated at 37 °C and liquid cultures were aerated by shaking at 180 rpm unless indicated otherwise.

Probes and inhibitors: The carmofur probes **1** and **2** were available from a previous study and their synthesis had been described.[9] Carmofur and 5-FU were purchased from Sigma.

Labeling with fluorescent ABP (1): After overnight growth on TSAMg plate or in liquid culture as indicated, bacteria were suspended to the desired density in TSB and added to microtubes in a final volume of 50–100 μL. For competitive ABPP experiments, the inhibitors (carmofur and 5-FU) were added from 100x-concentrated stock solutions in DMSO and pre-incubated with the cells for 60 min (37 °C, 300 rpm) prior to ABP-labeling. Compound **1** (1 μM) was added from a 100x stock solution in DMSO and cells were incubated for 60 min, at 37 °C, 300 rpm. After probe labeling, bacterial suspensions were transferred to 2 mL screw-cap tube filled with 30–50 μL of 4x SDS-Loading buffer and ca. 60–100 μL of 0.1 mm glass beads and lysed by bead-beating.

SDS-PAGE analysis of fluorescently labeled proteins: After adding the 4x SDS sample buffer (40% glycerol, 240 mM Tris·HCl pH 6.8, 8% SDS, 0.04% bromophenol blue, 5% β-mercaptoethanol), lysates of probe-labeled bacteria were boiled at 95 °C for 10 min and separated by SDS-PAGE gel. The gels were scanned for fluorescence in the Cy2 (488 nm) channel on a Amersham™ Typhoon™ 5 (cytiva).

ChemBioChem

Research Article
doi.org/10.1002/cbic.202300473

Chemistry Europe
European Chemical
Societies Publishing

Labeling with biotinylated probes and sample preparation for mass spectrometry: *S. aureus* USA300 JE2 cultures were grown on TSAMg for 24 h and resuspended to an OD_{600} ~20 in 3 mL TSB. For each biological replicate, 1 mL aliquots were transferred to a 1.5 mL tube and either carmofur–biotin (probe **2**; 2 μM) or an equal concentration of carmofur (as a control for nonspecific biological effects of the probe) were added, and cells were incubated for 60 min at 37 °C, 700 rpm before samples were spun down at 4500 g for 5 min at 4 °C, and the supernatant was aspirated. The cell pellets were resuspended in 1.2 mL RIPA lysis buffer (50 mM Tris, 150 mM NaCl, 0.1 % SDS, 0.5 % sodium deoxycholate, 1 % Triton X-100) and lysed by bead-beating. Samples were centrifuged for 5 min at 10 000 g at 4 °C. Protein concentration in the supernatant was adjusted to 1.0 mg mL^{-1}. Proteins were stored at −20 °C prior to sample preparation. For each sample, 50 μL streptavidin magnetic beads were washed twice with 1 mL RIPA lysis buffer and incubated with 1 mg protein from each sample with an additional 500 μL RIPA lysis buffer at 4 °C for overnight at 18 RPM rotator. After enrichment, beads were pelleted using a magnetic rack, and washed twice with RIPA lysis buffer (1 mL, 2 min at RT), once with 1 M KCl (1 mL, 2 min at RT), once with 0.1 M Na_2CO_3 (1 mL, ~10 s), once with 2 M urea in 10 mM Tris·HCl (pH 8.0; 1 mL, ~10 s), and twice with RIPA lysis buffer (1 mL per wash, 2 min at RT). After the final wash, the beads were transferred in 1 mL RIPA lysis buffer to fresh protein Lo-Bind tubes. Then, beads were washed three times in 500 μL 2 M/4 M urea, 50 mM ammonium bicarbonate (Ambic) with shaking for 7 min. Finally, beads were washed 3x with 500 μL of 50 mM Ambic with shaking for 7 min, each time transferring the samples to a new tube in-between washes. For on-bead digestion, 150 μL 50 mM Ambic, 3 μL 1 mM $CaCl_2$, 0.75 μL 1 M DDT, 4.5 μL 500 mM IAA and 6 μL MS grade trypsin solution were added and samples were incubated at 37 °C overnight at 800 rpm. Tryptic peptide digests were separated, and beads were washed with 70 μL 50 mM Ambic. For each sample, to the combined eluates received 20 μL of formic acid were added, and the samples were kept at −20 °C until analysis via LC–MS/MS.

LC–MS analysis: Varian's OMIX C18 tips were employed to perform sample cleanup and concentration. Peptide mixtures that comprised 0.1 % formic acid were loaded onto a Thermo Fisher Scientific EASY-nLC1200 system (C_{18}, 2 μm, 100 Å, 50 μm, 50 cm) and subjected to fractionation by using a 5–80 % acetonitrile gradient in 0.1 % formic acid at a flow rate of 300 nL min^{-1} for a duration of 60 min. The peptides that were separated were examined using a Thermo Scientific Orbitrap Exploris 480. Data was acquired in a data-dependent mode with the aid of a Top20 method. The raw data were processed by using the Proteome Discoverer 2.5 software, and the fragmentation spectra were searched against (*S. aureus* 300 LAC). Peptide mass tolerances of 10 ppm and a fragment mass tolerance of 0.02 Da were employed during the search. Peptide ions were filtered using a false discovery rate (FDR) set at 5 % for peptide identifications. To ensure accuracy, the filter criterion of two unique peptides was used, and three replicates were conducted for all samples. The protein abundance obtained from Proteome Discoverer was averaged across replicates, and the ratio of the ABPP-enriched sample versus the control tryptic digestion sample was calculated. Proteins enriched more than 1.5-fold by the biotinylated probe were selected. ABPP-enriched and other pull-down experiments are significantly limited by nonspecific binding.[36,37] The enrichment of these nonspecific proteins may be due to various reasons, such as naturally biotinylated proteins (e.g., carboxylase family proteins) and ribosomal proteins being enriched by streptavidin beads, as well as proteins with an affinity for hydrophilic beads being enriched. However, proteins exhibiting the latter two types of nonspecific binding were excluded. The mass spectrometry proteomics data

have been deposited to the ProteomeXchange Consortium via the PRIDE[38] partner repository with the dataset identifier PXD043275.

Antimicrobial activity testing: To determine the MIC, stock solutions of carmofur and 5-Fluorouracil were prepared at a concentration of 200 μM in sterile distilled water. These solutions were then diluted 1:2 in 96-well microtiter plates and inoculated with *S. aureus* strains at approximately $5×10^5$ CFU mL^{-1} in 100 μL. The 96-well microtiter plates were incubated overnight (18 h) to determine the MIC.[39]

Time–kill assay of carmofur/5-fluorouracil: A time–kill study was performed according to the Clinical and Laboratory Standards Institute guidelines following a method previously described.[40] In brief, 4×MIC (20 μM) of carmofur/5-fluorouracil was used to detect differences in time-dependent killing. Overnight cultures of *S. aureus* USA 300 JE2 were grown in Mueller–Hinton (MH) broth at 37 °C until the exponential phase was reached, indicated by $OD_{600} = 0.4$. The cells were then diluted to yield a final concentration of approximately $2×10^6$ cells per mL and transferred to a 50 mL tube containing 20 mL of MH broth, followed by the addition of appropriate concentrations of carmofur and 5-fluorouracil. Tubes were then incubated at 37 °C, and aliquots were removed at 0, 2, 4, 6, 24, 48, and 72 h for the determination of viable counts. Serial dilutions were prepared in sterile PBS and plated according to the method previously described. Colonies were counted after incubation of TSA plates at 37 °C for 16–22 h, with a detection level of $1×10^2$ CFU mL^{-1}.

Supporting Information

The authors have included Supporting Dataset 1 in the Supporting Information.

Acknowledgements

Conflict of Interests

The authors declare no conflict of interest.

Data Availability Statement

The mass spectrometry proteomics data have been deposited to the ProteomeXchange Consortium via the PRIDE partner repository with the dataset identifier PXD043275.

[1] A. C. M. van Esbroeck, A. P. A. Janssen, A. B. Cognetta III, D. Ogasawara, G. Shpak, M. van der Kroeg, V. Kantae, M. P. Baggelaar, F. M. S. de Vrij, H. Deng, M. Allarà, F. Fezza, Z. Lin, T. van der Wel, M. Soethoudt, E. D. Mock, H. den Dulk, I. L. Baak, B. I. Florea, G. Hendriks, L. De Petrocellis, H. S. Overkleeft, T. Hankemeier, C. I. De Zeeuw, V. Di Marzo, M. Maccarrone, B. F. Cravatt, S. A. Kushner, M. van der Stelt, *Science.* **2017**, *356*, 1084–1087.

[2] S. I. Van Kasteren, B. I. Florea, H. S. Overkleeft, *Methods Mol. Biol.* **2017**, *1491*, 1–8.

[3] S. Chakrabarty, J. P. Kahler, M. A. T. Van de Plassche, R. Vanhoutte, S. H. L. Verhelst in *Recent Advances in Activity-Based Protein Profiling of Proteases*, (Eds.: B. F. Cravatt, K.-L. Hsu, E. Weerapana), Springer International, Cham, **2019**, pp. 253–281.

[4] C. S. Lentz, *Biol. Chem.* **2020**, *401*, 233–248.

[5] H. J. Benns, C. J. Wincott, E. W. Tate, M. A. Child, *Curr. Opin. Chem. Biol.* **2021**, *60*, 20–29.

[6] M. Garland, J. J. Yim, M. Bogyo, *Cell Chem. Biol.* **2016**, *23*, 122–136.

[7] Y. Liu, M. P. Patricelli, B. F. Cravatt, *Proc. Natl. Acad. Sci. USA* **1999**, *96*, 14694–14699.

[8] C. S. Lentz, J. R. Sheldon, L. A. Crawford, R. Cooper, M. Garland, M. R. Amieva, E. Weerapana, E. P. Skaar, M. Bogyo, *Nat. Chem. Biol.* **2018**, *14*, 609–617.

[9] C. M. J. Ouairy, M. J. Ferraz, R. G. Boot, M. P. Baggelaar, M. van der Stelt, M. Appelman, G. A. Van der Marel, B. I. Florea, J. M. F. G. Aerts, H. S. Overkleeft, *Chem. Commun.* **2015**, *51*, 6161–6163.

[10] D. Pizzirani, C. Pagliuca, N. Realini, D. Branduardi, G. Bottegoni, M. Mor, F. Bertozzi, R. Scarpelli, D. Piomelli, T. Bandiera, *J. Med. Chem.* **2013**, *56*, 3518–3530.

[11] N. B. Doan, H. Alhajala, M. M. Al-Gizawiy, W. M. Mueller, S. D. Rand, J. M. Connelly, E. J. Cochran, C. R. Chitambar, P. Clark, J. Kuo, K. M. Schmainda, S. P. Mirza, *Oncotarget* **2017**, *8*, 112662–112674.

[12] J. Shelton, X. Lu, J. A. Hollenbaugh, J. H. Cho, F. Amblard, R. F. Schinazi, *Chem. Rev.* **2016**, *116*, 14379–14455.

[13] M. M. Islam, S. P. Mirza, *Drug Dev. Res.* **2022**, *83*, 1505–1518.

[14] W. B. Wang, Y. Yang, Y. P. Zhao, T. P. Zhang, Q. Liao, H. Shu, *World J. Gastroenterol.* **2014**, *20*, 15682–15690.

[15] D. B. Longley, D. P. Harkin, P. G. Johnston, *Nat. Rev. Cancer* **2003**, *3*, 330–338.

[16] S. Sato, T. Ueyama, H. Fukui, K. Miyazaki, M. Kuwano, *Gan to Kagaku Ryoho* **1999**, *26*, 1613–1616.

[17] N. Realini, C. Solorzano, C. Pagliuca, D. Pizzirani, A. Armirotti, R. Luciani, M. P. Costi, T. Bandiera, D. Piomelli, *Sci. Rep.* **2013**, *3*, 1035.

[18] A. Dementiev, A. Joachimiak, H. Nguyen, A. Gorelik, K. Illes, S. Shabani, M. Gelsomino, E. E. Ahn, B. Nagar, N. Doan, *J. Med. Chem.* **2019**, *62*, 987–992.

[19] N. Coant, W. Sakamoto, C. Mao, Y. A. Hannun, *Adv Biol Regul.* **2017**, *63*, 122–131.

[20] A. Rangel-Vega, L. Bernstein, E.-A. Mandujano Tinoco, S.-J. García-Contreras, R. García-Contreras, *Front. Microbiol.* **2015**, *6*, 282.

[21] N. S. Torres, J. J. Abercrombie, A. Srinivasan, J. L. Lopez-Ribot, A. K. Ramasubramanian, K. P. Leung, *Antimicrob. Agents Chemother.* **2016**, *60*, 5663–5672.

[22] A. Rangel-Vega, L. R. Bernstein, E. A. Mandujano-Tinoco, S. J. García-Contreras, R. García-Contreras, *Front. Microbiol.* **2015**, *6*, 282.

[23] C. Attila, A. Ueda, T. K. Wood, *Appl. Microbiol. Biotechnol.* **2009**, *82*, 525–533.

[24] C. Attila, A. Ueda, T. K. Wood, *Appl. Microbiol. Biotechnol.* **2009**, *82*, 525–533.

[25] F. Sedlmayer, A. K. Woischnig, V. Unterreiner, F. Fuchs, D. Baeschlin, N. Khanna, M. Fussenegger, *Nucleic Acids Res.* **2021**, *49*, e73.

[26] Y. N. Kang, A. Tran, R. H. White, S. E. Ealick, *Biochemistry* **2007**, *46*, 5050–5062.

[27] J. A. Brannigan, G. Dodson, H. J. Duggleby, P. C. E. Moody, J. L. Smith, D. R. Tomchick, A. G. Murzin, *Nature* **1995**, *378*, 416–419.

[28] M. Fellner, C. S. Lentz, S. A. Jamieson, J. L. Brewster, L. Chen, M. Bogyo, P. D. Mace, *ACS Infect. Dis.* **2020**, *6*, 2771–2782.

[29] V. Dalal, P. Kumar, G. Rakhaminov, A. Qamar, X. Fan, H. Hunter, S. Tomar, D. Golemi-Kotra, P. Kumar, *J. Mol. Biol.* **2019**, *431*, 3107–3123.

[30] M. M. Rahman, H. N. Hunter, S. Prova, V. Verma, A. Qamar, D. Golemi-Kotra, *mBio* **2016**, *7*, e02070–02015.

[31] K. Wu, Y. Xiu, P. Zhou, Y. Qiu, Y. Li, *Front. Pharmacol.* **2019**, *10*, 818.

[32] J. C. Powers, J. L. Asgian, O. D. Ekici, K. E. James, *Chem. Rev.* **2002**, *102*, 4639–4750.

[33] P. D. Fey, J. L. Endres, V. K. Yajjala, T. J. Widhelm, R. J. Boissy, J. L. Bose, K. W. Bayles, *mBio* **2013**, *4*, e00537–00512.

[34] M. Gélinas, L. Museau, A. Milot, P. B. Beauregard, *Microbiol. Spectr.* **2021**, *9*, e0080421.

[35] L. Maier, M. Pruteanu, M. Kuhn, G. Zeller, A. Telzerow, E. E. Anderson, A. R. Brochado, K. C. Fernandez, H. Dose, H. Mori, K. R. Patil, P. Bork, A. Typas, *Nature* **2018**, *555*, 623–628.

[36] S. Wang, Y. Tian, M. Wang, M. Wang, G.-b. Sun, X.-b. Sun, *Front. Pharmacol.* **2018**, *9*.

[37] S. E. Tully, B. F. Cravatt, *J. Am. Chem. Soc.* **2010**, *132*, 3264–3265.

[38] Y. Perez-Riverol, J. Bai, C. Bandla, D. García-Seisdedos, S. Hewapathirana, S. Kamatchinathan, D. J. Kundu, A. Prakash, A. Frericks-Zipper, M. Eisenacher, M. Walzer, S. Wang, A. Brazma, J. A. Vizcaíno, *Nucleic Acids Res.* **2022**, *50*, D543–d552.

[39] G. Kahlmeter, D. F. J. Brown, F. W. Goldstein, A. P. MacGowan, J. W. Mouton, I. Odenholt, A. Rodloff, C. J. Soussy, M. Steinbakk, F. Soriano, O. Stetsiouk, *Clin. Microbiol. Infect.* **2006**, *12*, 501–503.

[40] F. Silva, O. Lourenço, J. A. Queiroz, F. C. Domingues, *J. Antibiot. (Tokyo).* **2011**, *64*, 321–325.

[41] B. Arsic, Y. Zhu, D. E. Heinrichs, M. J. McGavin, *PLoS One* **2012**, *7*, e45952.

RESEARCH ARTICLE
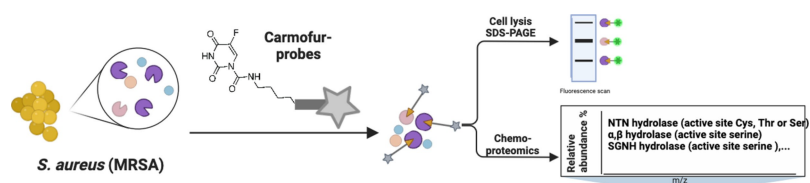
Enzyme targets of activity-based probes built on the anti-neoplastic drug and antimicrobial agent carmofur in methicillin-resistant *Staphylococcus aureus* (MRSA) have been identified. Chemoproteomic profiling revealed a broad reactivity of the probe against both cysteine and serine hydrolases, and identified un-characterized bacterial enzymes; this has implications for putative human or microbial (off)targets engaged by therapeutic use of carmofur in the clinic.

M. J. Uddin, Prof. Dr. H. S. Overkleeft, Prof. Dr. C. S. Lentz

1 – 10

Activity-Based Protein Profiling in Methicillin-Resistant *Staphylococcus aureus* Reveals the Broad Reactivity of a Carmofur-Derived Probe